Stationary states of Toom cellular automata in simulations

Danuta Makowiec*
Institute of Theoretical Physics and Astrophysics, Gdańsk University, ulica Wita Stwosza 57, 80-952 Gdańsk, Poland
(Received 21 September 1998; revised manuscript received 7 June 1999)

Stationary states of Toom probabilistic cellular automata are tested in computer experiments. The aim of the tests is to identify the features characterizing the equilibrium states understood as in statistical mechanics. Namely, we investigate the following: scaling laws that involve critical parameters β, γ, and ν, locality of the interactions, and density of the relative entropy between stationary states. The arguments showing that stationary Toom states are not the equilibrium ones are provided. [S1063-651X(99)12310-9]

PACS number(s): 05.50.+q, 05.70.Jk

I. INTRODUCTION

The Monte Carlo approach to emulate the canonical ensemble in computer simulations is one of the most powerful techniques among the computer methods developed for statistical physics during the recent years. This approach provides not only the estimates for thermodynamic functions, but also offers special insight into the local interactions. It means that we have the opportunity to examine links between the microdynamics and resulting equilibrium systems [1–3]. The famous two-dimensional Ising system is widely known as the equilibrium–statistical-mechanics system that models the ferromagnetic phenomena. There is much effort focused on testing of various computer algorithms which would reproduce a system with the Ising-Lenz interactions. Such algorithms are called kinetic Ising models.

The proposition originating from extended dynamical systems like cellular automata, or coupled map lattices, is qualitatively distinct from the mentioned kinetic models. The evolution of these systems, i.e., lattices of interacting dynamical systems with discrete (cellular automata [4–6]) or continuous (coupled map lattices [7,8]) phase space, is governed by the set of local dynamical rules instead of local energy, which is used in kinetic Ising models. Moreover, the changes on a lattice configuration are synchronized, which results in a discrete time evolution, while in kinetic Ising models the computer algorithms allow techniques that simulate the continuous time. The main goal of the study of extended dynamical systems is to find the relationship between the investigated system and the equilibrium one. In particular, one searches for meaning of the basic statistical-mechanic notions such as energy, specific heat, temperature, etc., one also looks for mechanisms that govern the critical phenomena, [9,10]. In the case when a local rule is not reversible the results are by no means obvious [6–8]. Little is known about the nature of the stationary phase-space measures in the nonergodic regime, especially when there is more than one stationary measure.

In the following, we concentrate on cellular automata with Toom local rule (TCA) as the alternative to kinetic Ising models. Despite intensive investigations both on the rigorous level [5,10,11] and on the experimental one [4,12,13], the properties of the thermodynamic system that arise from Toom probabilistic cellular automata are still unclear.

It is commonly believed that if the stationary measure of any stochastic system satisfies the detailed balance condition, then its stationary evolution generates a random walk on the configuration space weighted by some Gibbs distribution [14]. Gibbs measures are the central objects of the rigorous classical statistical mechanics. The fact that a probability measure μ is a Gibbs one implies that the finite-volume conditional expectation values are determined by Hamiltonians that are defined as sums of local interactions (see [15] for details).

The problem of Gibbsianness of stationary states for cellular automata is simplified due to the so-called dichotomy theorem [6]. An immediate consequence of this theorem is that for cellular automata dynamics satisfying the detailed balance condition, all invariant measures are Gibbsian. However, the problem whether the detailed balance is a necessary or satisfactory condition for a system to be an equilibrium one is still open [16].

There are reasons [10] to think that although transition rates arising from the stationary Toom probabilistic cellular automata do not satisfy the detailed balance condition, the system is the equilibrium one. Strictly speaking, the stationary measure is then the Gibbs measure. The idea that cellular automata with Toom stochastic evolution lead to an equilibrium system is based on the following. First, it is due to similarity of TCA to Domany probabilistic cellular automata, which are known to create the well-defined equilibrium system (see, e.g., [5]). Second, to the presence of the so-called eroder property, which means that any finite island of one phase surrounded by the sea of the other phase will decay in finite number of time steps [11].

In the following section we recall the concept Domany PCA and give the definition of the investigated TCA. This is done in a way that the relation between these two models is easily seen. We also give some insights into the mechanism of self-establishing stationary islands of the phase opposite to the one in the neighborhood.

TCA are known to be a nonergodic system for certain model parameters [4–6,11]. Then the critical behavior similar to the continuous phase transition can be studied. If the symmetry of the interactions is the same as in the Ising model, then it is generally conjectured that the considered

*Electronic address: fizdm@univ.gda.pl

stochastic system belongs to the Ising universality class [17]. This seems to be valid regardless of the nature of thermodynamic system (whether or not it is an equilibrium one). In Sec. III we discuss whether TCA belong to the Ising universality class. Our results seem to indicate that this is not true. However, we show that Toom cellular automata exhibit the similar critical behavior to the two-dimensional coupled map lattices with synchronized dynamics [8].

In Sec. IV we give arguments, supported by the computer experiments, that in case of the periodic TCA the stationary measure is not the Gibbsian one. The two basic features of Gibbsian measures, the quasilocality of interactions and vanishing of the relative entropy density between stationary measures, are violated in the critical regime.

II. TOOM VERSUS DOMANY CELLULAR AUTOMATA

Both dynamical systems considered here, Toom and Domany CA, are defined on a square, two-dimensional lattice, with discrete local variables: spins $\sigma_i(t)$ are assigned to each node of a lattice, index i denotes square lattice coordinates, while t denotes the discrete time. Spin may take one of the two values, i.e., $\sigma_i(t) \in \{-1,+1\}$. The state of any spin is determined by states of its three nearest neighbors, named N_i, E_i, C_i. The neighbors are chosen as follows:

$$\begin{array}{ccccccc} & | & & | & & | & \\ - & . & - & N_i & - & . & - \quad . \\ & | & & | & & | & \quad . \\ - & . & - & C_i=\sigma_i & - & E_i & - \quad . \\ & | & & | & & | & \end{array} \tag{1}$$

At each time step t, states of all spins are updated synchronously according to the following evolution rule. Let $\Sigma_i = N_i + E_i + C_i$. Then, in the Toom system,

$$\sigma_i(t+1) = \begin{cases} \operatorname{sgn}\Sigma_i & \text{with probability } \frac{1}{2}(1+\varepsilon) \\ -\operatorname{sgn}\Sigma_i & \text{with probability } \frac{1}{2}(1-\varepsilon). \end{cases} \tag{2}$$

The parameter $\varepsilon \in [0,1]$ mimics the stochastic temperature effects. $\varepsilon = 1$ means completely deterministic evolution, i.e., temperature $T=0$, while $\varepsilon = 0$ corresponds to the fully random rule, i.e., temperature $T=\infty$. Hence, ε can be seen as related to thermodynamic temperature via the following relation:

$$\varepsilon \to \tanh\frac{1}{T}. \tag{3}$$

In the Domany system,

$$\sigma_i(t+1) = \begin{cases} \operatorname{sgn}\Sigma_i & \text{with probability } \begin{cases} 1-\varepsilon_1^D & \text{for } |\Sigma_i|=1 \\ 1-\varepsilon_3^D & \text{for } |\Sigma_i|=3 \end{cases} \\ -\operatorname{sgn}\Sigma_i & \text{with probability } \begin{cases} \varepsilon_1^D & \text{for } |\Sigma_i|=1 \\ \varepsilon_3^D & \text{for } |\Sigma_i|=3, \end{cases} \end{cases}$$

with $\varepsilon = 1/T$ the inverse temperature parameter given as

$$\varepsilon_1^D = \frac{1}{2}(1-\tanh\varepsilon) \quad \text{and} \quad \varepsilon_3^D = \frac{1}{2}(1-\tanh 3\varepsilon).$$

Thus, one notices two ''temperatures'' appearing in the Domany model. The lower temperature ε_3^D characterizes spins that form aligned clusters, while the higher temperature ε_1^D is assigned to areas with spins forming neighborhoods of spins in different states. So, the temperature acts as if ''kicking'' more frequently in the mixed neighborhoods than in the uniform clusters.

In this paper we study properties of the Toom system via computer experiments. Hence, we deal only with finite lattices. Therefore, we have to supplement the evolution rule (2) with some boundary conditions. By introducing the periodic boundary conditions the resulting system becomes infinite: it falls into the class of periodic thermodynamic systems with a period equal to $L \times L$ [18]. Phenomena such as phase transitions, are observed in such infinite systems, though it follows from the rigorous studies that a thermodynamic system which arises from periodic ones in the limit of $L \to \infty$, remembers the periodicity of each element of the sequence [19]. Hence, the limit of periodic TCA differs from the general unconditional thermodynamic Toom cellular automata.

Almost all of the presented results are based on the data obtained in the following experiment. At time $t=0$ states of all spins are aligned, namely, are set to $+1$. Then, for later times the evolution rule (2) is employed with some ε. The stochasticity of the system is driven by the family of standard functions accessible in the C ANSI running under the HP-UNIX system. These functions generate pseudorandom numbers by using the well-known linear congruential algorithm and 48-bit integer arithmetic.

The evolving system is given some time to reach the stationary state. In the case of small lattices ($L \leqslant 100$) this time is taken to be $100L$ for all values of ε. Such time intervals are sufficient to find the system in the steady state. For large systems: $L=200$ or $L=300$, to ensure that the observed statistical properties do indeed correspond to the stationary regime, we wait until differences in the magnetization averaged over 500 time steps are negligible. At the critical regime it takes about 30 000 time steps.

When the system is in a stationary state, then at each time step a macroscopic observable A is computed according to a present microscopic state of a lattice,

$$A(t) = A(\{\sigma_i(t)\}_{i=1,\ldots,L^2}). \tag{4}$$

Next, to decrease the influence of the local fluctuations, $A(t)$ is averaged along a trajectory of some length T (usually $T = 10\,000$), i.e.,

$$\hat{A} = \frac{1}{T}\sum_{t=1,\ldots,T} A(t). \tag{5}$$

To avoid the possibility that the examined state is attracted by some metastable state, we perform N independent experiments, with N in the range $100,\ldots,1800$. Therefore, the final ensemble average for an observable A is given as

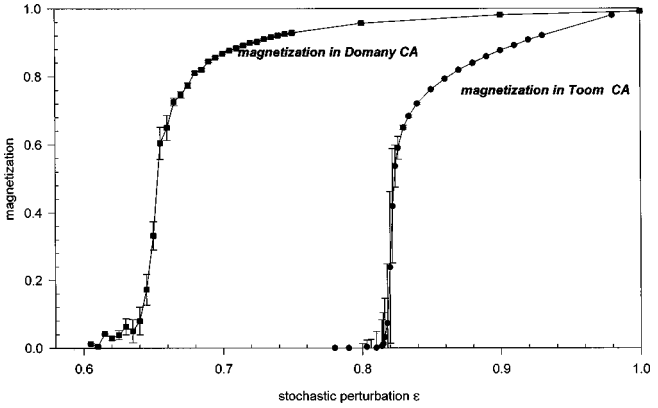

FIG. 1. Decay of the magnetization $\langle m \rangle$ in Toom CA (dots) and Domany CA (squares). The regimes ''ferromagnetic'' ($\langle m \rangle \gg 0$), and ''paramagnetic'' ($\langle m \rangle \approx 0$) are separated by the region of critical changes. Notice the increase of standard deviation errors, marked by error bars, in the region of the phase transition.

$$\langle A \rangle = \frac{1}{N} \sum_{k=1,\ldots,N} \hat{A}^{(k)}, \tag{6}$$

where $\hat{A}^{(k)}$ means the average of an observable A in the sense of Eq. (5) obtained in the $k-$th experiment.

Since we focus attention on the continuous phase transition of the Ising-like type, we concentrate on the following observables:

(i) The magnetization $\langle m \rangle$, which according to Eq. (4) is defined as

$$m(t) = \frac{1}{L^2} \sum_{i=1,\ldots,L^2} \sigma_i(t). \tag{7}$$

(ii) The magnitude of the magnetization, denoted by $\langle |m| \rangle$, is calculated from Eq. (6) as

$$\langle |m| \rangle = \frac{1}{N} \sum_{k=1,\ldots,N} \left(\frac{1}{T} \sum_{t=1,\ldots,T} |m(t)| \right)^{(k)}. \tag{8}$$

These two functions are the standard order parameters exploited in studies of ferromagnetic, Ising-type systems on finite lattices [1].

In both systems, Toom and Domany, depending on the stochastic perturbation strength ε, two qualitatively distinct regimes are observed (Fig. 1). For values smaller than the critical temperature, denoted by ε_{cr}, the systems are of the *paramagnetic* type, since up and down spins are equiprobable. Above ε_{cr} the initial state phase $(+)$ dominates, which implies the positive total magnetization.

The snapshots taken close to the transition show the formation of clusters of aligned spins of the $(-)$ phase surrounded by the sea of pluses; see Fig. 2. Notice that all clusters are islands with a characteristic triangular shape that mirrors the triangle of the basic neighborhood (1). In the purely deterministic Toom CA ($\varepsilon = 1$) the eroder property causes the decay of the clusters of such kind in a few time steps. However, when the stochastic perturbation is present, these islands can live for a long time. This is because the eroding process attacks any triangle-shaped island through its edge made of North and East neighbors, only. The two

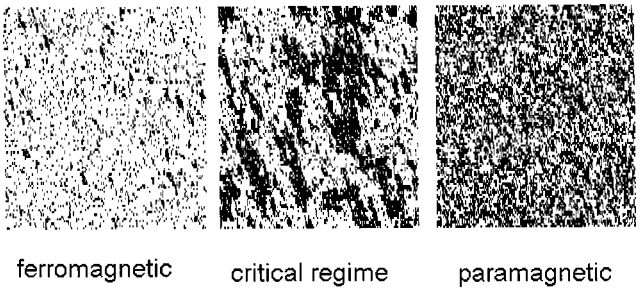

FIG. 2. Typical snapshots of TCA, in time asymptotic regions, observed for a linear size lattice $L = 200$. Up- and down-spins are represented by white and black pixels, respectively. (a) Ordered ''ferromagnetic'' phase $\varepsilon = 0.90$, (b) Critical regime $\varepsilon = 0.82$, (c) Disordered ''paramagnetic'' phase, $\varepsilon = 0.60$.

other edges that go vertically and horizontally have a property of free wandering. Any perturbation that affects a spin from these edges produces a free propagating change which enlarges the cluster size. Hence, the island phase leaks outside the cluster towards West or South directions. As the result of both these processes we observe the shift of the cluster in the West-South direction. Hence, in the case of TCA there is no need to manipulate the temperatures to protect clusters of aligned spins, as is done in the case of Domany CA. However, the Toom mechanism of protecting islands of a given phase is weaker than in the Domany one, since the value of ε_{cr} in Toom model strongly differs from the value of ε_{cr} in Domany model (see Fig. 1).

The development of spin spatial dependencies can be analyzed by the two-point spatial correlation function $C_{\mathbf{v}}(r)$ defined along the direction $\mathbf{v}$, and for r being the spatial separation of two points. $C_{\mathbf{v}}(r)$ is given as

$$C_{\mathbf{v}}(r) = \frac{\langle \sigma_0 \sigma_{r\mathbf{v}} \rangle - \langle \sigma_0 \rangle^2}{1 - \langle \sigma_0 \rangle^2}. \tag{9}$$

The exponential decay of the correlation function leads to the natural definition of the correlation length $\xi_{\mathbf{v}}$ along the $\mathbf{v}$ direction.

In Toom CA the spatial extension of newborn clusters of aligned spins in the ferromagnetic regime (for $\varepsilon > \varepsilon_{cr}$) is of the order of one or two lattice units in any direction $\mathbf{v}$. The system is thus isotropic. However, close to the transition point the data show the formation of nonisotropic large-scale dependencies; see Fig. 3. The correlation lengths extracted from the estimations of the exponential decay of $C_{\mathbf{v}}(r)$ for the basic three directions from the origin to East-South, West-South, and East are $\xi_{ES} \approx 22 \pm 2$, $\xi_{WS} \approx 12 \pm 1$, and $\xi_E \approx 15 \pm 2$, respectively. The distance r is calculated in Pitagorean metric. The strong correlation between spins emerges sharply in the system when we approach ε_{cr} from the ferromagnetic side and decay smoothly when passing through towards the paramagnetic regime. Eventually, when $\varepsilon < 0.600$ (in the case of $\varepsilon \ll \varepsilon_{cr}$), then the system becomes isotropic again with the correlation spreaded over a few lattice steps; see [12] for details.

III. CRITICAL PROPERTIES OF TCA

As we have seen in the preceding section, the critical regime in TCA manifests itself in the way characteristic for

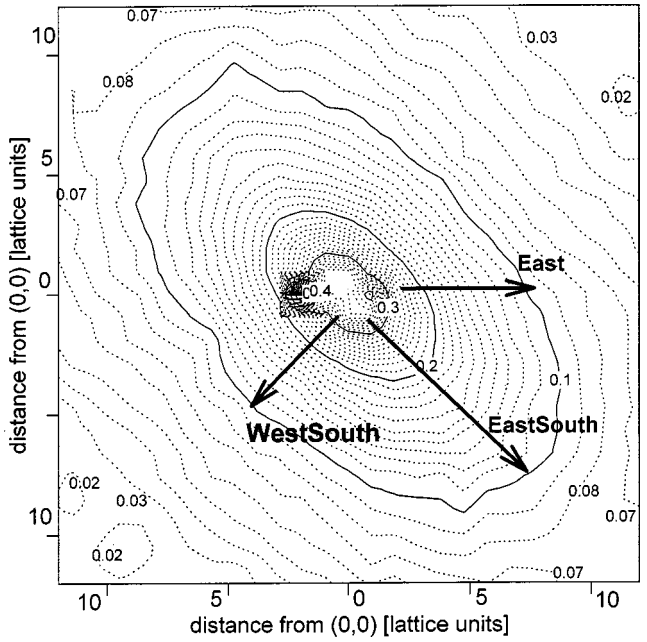

FIG. 3. Two-point correlation function of magnetization obtained on the lattice with $L=200$ at $\varepsilon=0.820$ (the contour plot). EastSouth, WestSouth, and East denote the basic three directions for the correlation dependence.

any thermodynamic system, i.e., by the increase of correlation between spatially separated spins. This signals the occurrence of continuous phase transition.

The standard order parameter for the ferromagnetic phase transition is the magnetization, defined by Eq. (7). To avoid some finite-size lattice effects the magnitude of the magnetization, defined by Eq. (8), is convenient to be considered as the order parameter. The susceptibility $\langle\chi\rangle$ is the other function that characterizes the continuous phase transition. Due to the relation between fluctuations of the magnetization and the linear response of the magnetization to any change of an external (temperature) parameter, we have the following general formula for the susceptibility [3]:

$$\langle\chi\rangle\propto\langle m^2\rangle-\langle m\rangle^2,$$

which in the case of a finite-size lattice becomes

$$\langle\chi_L\rangle=L^2(\langle m^2\rangle-\langle|m|\rangle^2). \tag{10}$$

In the equilibrium thermodynamic system close to the phase transition both magnetization and susceptibility depend algebraically on the distance to the critical point [3]. Following this observation the corresponding power laws are expected to apply to TCA in the infinite-size limit. Namely, when stochastic perturbation reaches its critical value ε_{cr}, magnetization, susceptibility, and the correlation length should exhibit the following properties:

$$\langle m\rangle\propto(\varepsilon-\varepsilon_{cr})^{\beta} \text{ for } \varepsilon>\varepsilon_{cr},$$

$$\langle\chi\rangle\propto(\varepsilon-\varepsilon_{cr})^{-\gamma} \text{ for } \varepsilon\to\varepsilon_{cr},$$

$$\langle\xi\rangle\propto(\varepsilon-\varepsilon_{cr})^{-\nu} \text{ for } \varepsilon\to\varepsilon_{cr} \tag{11}$$

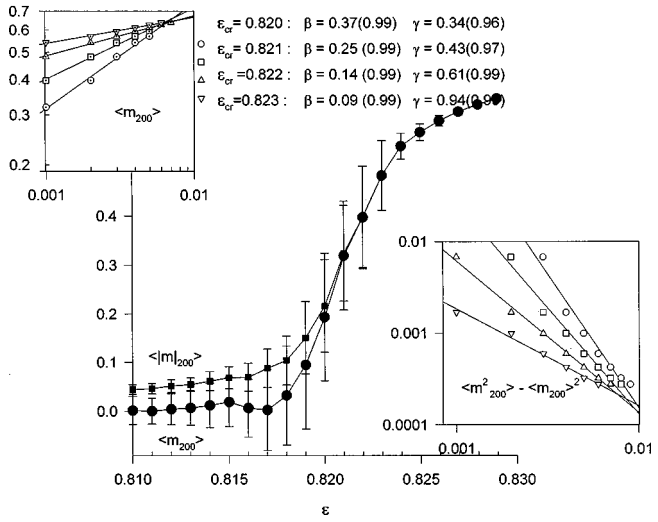

FIG. 4. Direct measure of β_{200} and γ_{200} on the large lattice $L=200$. Plots of $\langle m\rangle$ (dots) and $\langle|m|\rangle$ (squares) are presented as a function of ε. Different β_{200}'s and γ_{200}'s are estimated for the subsequent choice of ε_{cr}: 0.820, 0.821, 0.822, and 0.823 by linear fits on log-log plots (small windows).

and where β, γ, and ν are the usual, static critical exponents. The importance of the characterization of the critical changes by critical exponents lies in the fact that the set of the exponents determines the universality class.

As the first step in obtaining the critical exponents for Toom system, we extract β_L and γ_L for the periodic system, directly from the experiments with a large ($L=200$), though a finite lattice. Figure 4 presents our results. Since we do not know the exact value for the transition point, we fix it, in turn as $\varepsilon_{cr}=0.820$, 0.821, 0.822, and 0.823. The log-log dependence of magnetization and susceptibility on the distance to the criticality is expected to be linear. In Fig. 4 small windows depict the log-log scatter plots of the considered functions. In Fig. 4 the bars of the standard deviation errors for the presented data are included to show that although the size of the lattice is large, we obtain a large variety of results.

The quality of our linear fit coefficients is estimated by the standard correlation coefficient r^2. If $\{(x_i,y_i),i=1,\ldots,n\}$ are the n data points for which the linear relationship is sought, then denoting by s_{xx} and s_{yy} the sample variance, i.e.,

$$s_{xx}=\frac{1}{n-1}\sum_i (x-\langle x\rangle)^2, \quad s_{yy}=\frac{1}{n-1}\sum_i (y-\langle y\rangle)^2$$

and by s_{xy} the sample covariance, i.e.,

$$s_{xy}=\frac{1}{n-1}\sum_i (x-\langle x\rangle)(y-\langle y\rangle),$$

we obtain the following formula for the correlation coefficient r:

$$r=\frac{s_{xy}}{\sqrt{s_{xx}s_{yy}}}.$$

The correlation coefficient measures the strength of a linear relationship between x and y variables. r^2 takes its maximal value 1 only when all the points of the scatter plot lie exactly on a straight line. The slope of this line is given as

$$b=\frac{s_{xy}}{s_{xx}}.$$

r^2 takes its minimal value 0 when there is no linear relation between x and y. In the following, all linear fits together with the corresponding correlation coefficients are calculated by the computer program SIGMAPLOT, Scientific Graphic Software version 2.01, designed by the Jandel Corporation.

Our data imply that exponents are best consistent with the Ising universality class when $\varepsilon \in (0.822,0.823)$ and then they are $\beta_L \approx 0.1$ and $\gamma_L \approx 0.9$. Nevertheless, these results are far from the characteristic of the Ising system. However, they hint that in the thermodynamic limit of the infinite lattice size, we can expect well-defined power law behavior.

The reliable values for quantities β, γ, and ν for the infinite lattice size are accessible by finite-size lattice studies [20,21]. Based on the fact that at criticality the correlation length ξ attains the lattice size L, i.e., $\xi \approx L$, the finite-size scaling theory provides the measure for power law behavior of any observable. It follows that the value of any finite-lattice-size observable taken at the infinite-size transition point, named ε_{cr}^*, scales with the lattice size. For magnetization and susceptibility, the finite-lattice-size theory provides the relations

$$\langle |m(\varepsilon_{cr}^*)| \rangle \propto L^{-\beta/\nu},$$

$$\langle \chi_L(\varepsilon_{cr}^*) \rangle \propto L^{\gamma/\nu-2}. \tag{12}$$

The transition point ε_{cr}^* can be determined independently of the other quantities by using Binder's method [8,20]. Binder's method is based on the fact that the fourth order cumulants of the magnetization, i.e., family of functions defined for a given L by the formula

$$U_L(\varepsilon)=1-\frac{\langle m^4 \rangle}{3\langle m^2 \rangle^2} \tag{13}$$

are expected to intersect each other at the unique point ε_{cr}^*, which is independent of L.

In Fig. 5 we present our estimates of ε_{cr}^* for TCA. From the sample data we calculate the scatter points for cumulants U_L versus ε for system sizes ranging from $L=20$ to 100. Then we interpolate these points by straight lines. By an eye inspection we see that the common unique intersection point for all curves falls within the interval $\varepsilon_{cr}^* \in (0.8220,0.8224)$. Since the step of the tuning parameter ε in our experiments is $\Delta=0.001$, the best approximation for ε_{cr}^* is $\varepsilon_{cr}=0.8222$. Thus, our further estimates have the systematic error produced by some uncertainty in the choice of ε_{cr}. One can notice that the common value of the cumulants at the critical point is $U_L(\varepsilon_{cr}) \approx 0.6067$ and this value is close to the corresponding one found for the systems from Ising universality class, $U_{Ising} \in (0.610,0.612)$ [8].

Having found ε_{cr} we can proceed further to estimate ν, the critical exponent that is responsible for divergence of the correlation length ξ at criticality; see Eq. (11). In order to measure ν we take advantage of the scaling properties of cumulants U_L,

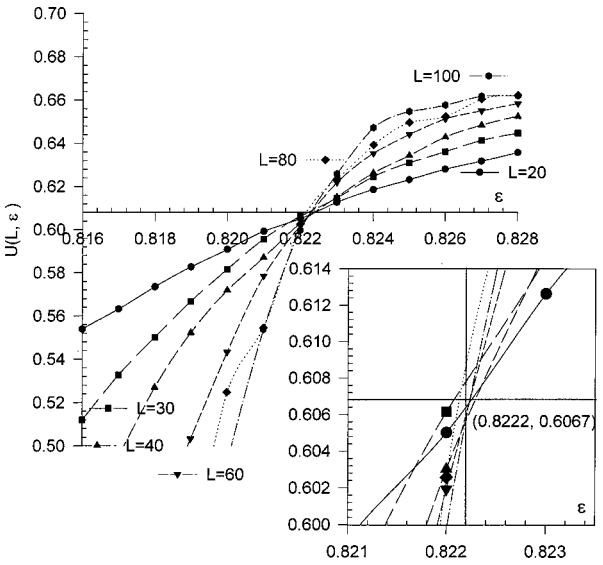

FIG. 5. Estimates for ε_{cr} by Binder's method. Plots of cumulants versus ε are presented for system sizes: $20 \leqslant L \leqslant 100$. Symbols correspond to raw data, lines to spline connections of these points to determine the intersection region (the small window).

$$\frac{dU_L}{d\varepsilon}(\varepsilon_{cr}) \propto L^{1/\nu}, \tag{14}$$

as well as the properties of logarithmic derivatives of the higher moments of magnetization, namely,

$$\frac{d\log\langle |m| \rangle}{d\varepsilon}(\varepsilon_{cr}), \quad \frac{d\log\langle m^2 \rangle}{d\varepsilon}(\varepsilon_{cr}), \quad \frac{d\log\langle m^4 \rangle}{d\varepsilon}(\varepsilon_{cr}). \tag{15}$$

All of them obey the same scaling as the cumulants.

To estimate numerically the derivatives in Eqs. (14) and (15) we use the standard finite centered difference formula. We apply this formula for a pair of neighboring points ε and $\varepsilon+\Delta$ to obtain the approximate derivative at $\varepsilon+\frac{1}{2}\Delta$. The error coming from the centered difference formula is Δ^2 since all derivatives are linear in the interval of $\varepsilon \in (0.820,\ 0.825)$. Knowing the linear dependence of the approximate derivative we calculate the interpolating value at $\varepsilon_{cr}=0.8222$ for each of the considered functions. The obtained data are presented in Fig. 6. Our results yield $\nu \approx 0.85 \pm 0.02$. Since the error of the numerical derivation is negligible when compared to the systematic error coming from the uncertainty of the position of the infinite-size critical point, we estimate the error interval by comparing the found value of ν to the estimates obtained if $\varepsilon_{cr}=0.822$ is considered.

Having estimated the value of ν we can proceed to measure β and γ according to Eq. (12). Again, for the considered functions $|m|$, m^2, and m^4 we apply the linear interpolation to calculate values of these functions at the critical point $\varepsilon_{cr}=0.8222$. These results are presented in Fig. 7.

To sum up, let us compare the characteristic features of the critical behavior of TCA to the corresponding quantities

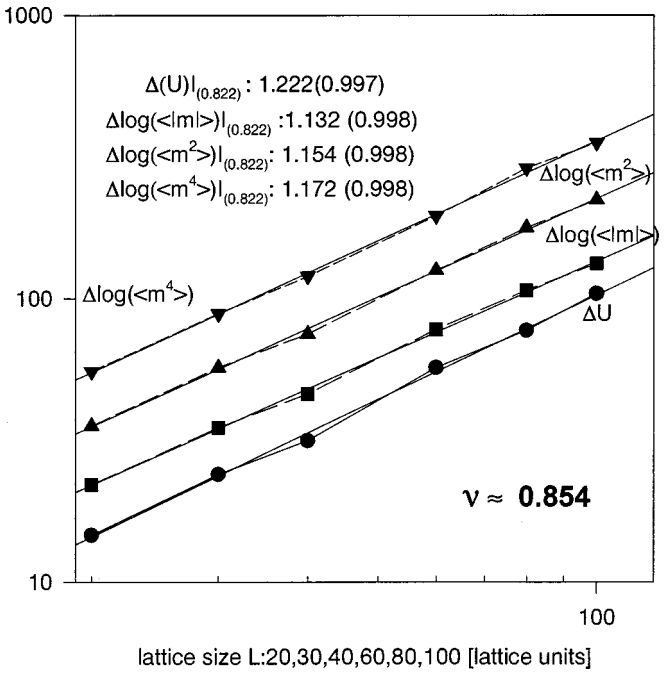

FIG. 6. Estimates for ν in TCA via the finite-size theory from, the slope of derivative of the 4th order magnetization cumulant at critical point U; the slope of the logarithm derivatives of $\langle|m|\rangle$, $\langle m^2\rangle$, and $\langle m^4\rangle$ [see Eq. (15)] at the critical point. Data collected in $1400,\ldots,120$ experiments with lattices $L=20,\ldots,100$ respectively are presented on log-log plots. The numbers in ( ) mean the correlation coefficients r^2 for the corresponding linear fits.

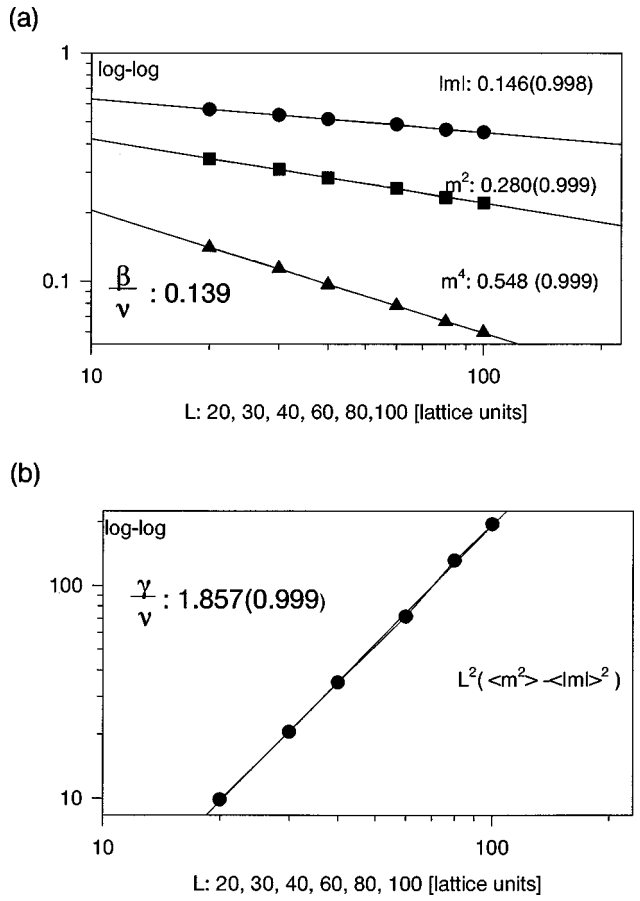

FIG. 7. Estimates for (a) β and (b) γ in TCA via the finite-size scaling: (a) β/ν from $\log(\langle|m(\varepsilon_{cr})|\rangle)(L)$, $\log(\langle m^2(\varepsilon_{cr})\rangle)(L)$, and $\log(\langle m^4(\varepsilon_{cr})\rangle)(L)$; (b) γ/ν from $\log L^2[\langle m^2(\varepsilon_{cr})\rangle(L)-\langle|m(\varepsilon_{cr})|\rangle^2(L)]$. The log-log plots.

in other two-dimensional (2D) ferromagnetic systems: rigorous quantities of the two-dimensional Ising system and exponents in synchronized coupled map lattice,

	β	γ	ν
TCA	0.12	1.59	0.85
Ising (2D)	0.125	1.75	1
CML [8]	0.115	1.55	0.89

(16)

The difference between values of the exponents, especially in γ and ν, for the Ising and Toom systems suggests that TCA do not belong to the Ising class of universality. But one can find the relationship between TCA and the synchronized coupled map lattices: the first and third line of Eq. (16). In the case of CML it is stressed [8] that the exponent ratios β/ν and γ/ν do take the Ising system values. This fact places the CML system in the weak-Ising universality class. For the Toom system we have $\beta/\nu=0.139$ and $\gamma/\nu=1.857$; see Fig. 7. Both ratios are rather different from the corresponding exponents of Ising system.

Before stating any final conclusion, however, we have to consider errors. Besides the systematic error stemming from our truncation of ε_{cr}, we have a constant source of statistical errors. The expectation values of the magnitude of magnetization (see Figs. 1 and 4) carry the standard deviation errors of 15 to 25 % independently of the system size. Such large errors are expected to occur since we are in the dynamical region of ergodicity breaking and symmetry breaking. Fortunately, all linear regression coefficients calculated according to our mean values show the perfect relationship. Therefore, we are sure that our results are reliable, though errors do not allow us to provide more significant digits in the presented numbers.

The above discussion supports our final statement that TCA and CML do belong to the same universality class, although the weak-Ising class membership in case of TCA is not clear: the Toom exponents only roughly satisfy the hyperscaling relation that is characteristic for Ising and weak-Ising systems: $2\beta+\gamma=2\nu$.

In traditional experimental work (not computer simulations) the types of continuous phase transitions are distinguished by the shape of curves, which represent the specific heat dependence on temperature [22,23]. In the Ising phase transition the left wing of the curve of the specific heat, corresponding to $T=0$, must take significantly lower values than its right wing. The opposite case, when the specific heat is much higher before the phase transition than after it, is the characteristic feature of the, so-called, diffusive phase transition.

Since in our case the concept of thermodynamic free energy is undefined, we evaluate the specific heat by assuming that the energy density of the system is proportional to the density of nonclustered spins. This idea arises from the famous Pirogov-Sinai theory according to which the energy of a lattice state is carried by the contours that surround pure phase clusters [15,18]. We estimate the energy density in

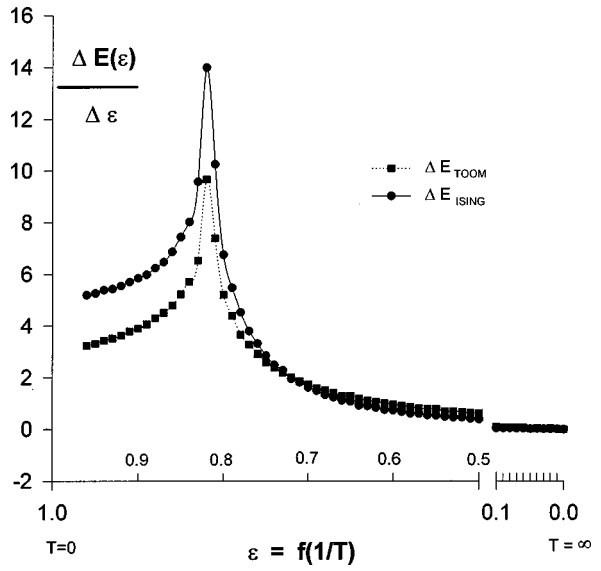

FIG. 8. Specific heat vs temperature T [see Eq. (3)] for Toom PCA. The specific heat is calculated as a change in the energy density caused by the small change of temperature at the given temperature. The obtained shape hints at the diffusive mechanism of the phase transition.

TCA stationary states in two ways: (1) a nonclustered spin means a spin for which the Toom neighborhood (1) is not homogeneous, and (2) a nonclustered spin means a spin for which the Ising neighborhood (i.e., the four spins surrounding the central spin and the central spin itself) is not homogeneous.

The results are presented in Fig. 8. Thus, the phenomenological classification of the continuous phase transitions based on the shape of the specific heat curve suggests that the Toom system undergoes the phase transition of the diffusive type.

IV. GIBBSIANNESS OF TCA

The last question we would like to address is whether TCA are the equilibrium system. We will seek the answer by checking if their stationary measure is a Gibbs one. If the stationary state is Gibbsian, then for any finite configuration $\{\sigma_\Lambda\}$, $\ln \mu(\sigma_\Lambda)$ exists and represents the energy of the configuration $\{\sigma_\Lambda\}$. Since in TCA the existence of steady clusters of aligned spins is closely related to the appearance of corresponding vertical and horizontal lines of such spins, we can expect that the energy carried by the configurations is determined by the linear size of a cluster rather than by its volume. This would suggest that the dynamics of the TCA generates the feature typical for the Ising interactions.

There are two basic features that characterize a Gibbs measure [6,10,15,16]: quasilocality of interactions, which means that the finite-volume conditional probabilities are continuous with respect to the external conditions, and vanishing of the relative entropy density between stationary measures arising from the same interactions.

In this section no attempt is made to provide error bars on values presented. Errors may arise from a combination of finite-size effects, finite equilibration time effects, and systematic deviations due to the choice of the measurement procedure.

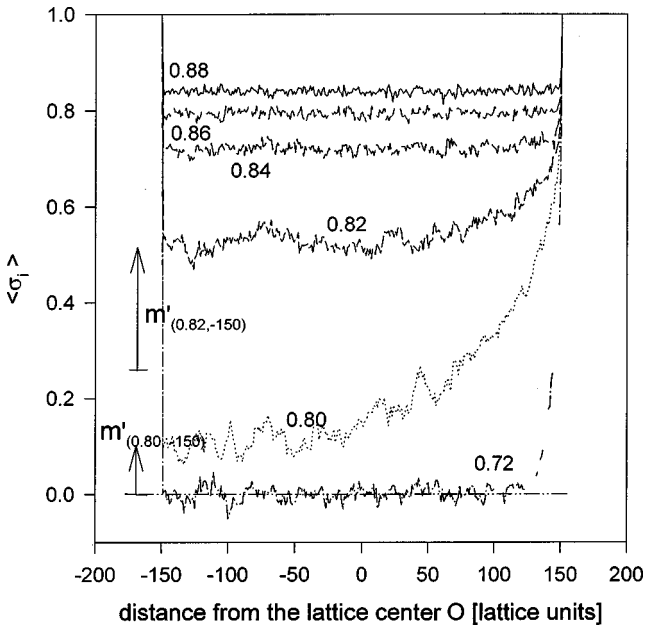

FIG. 9. Influence of boundary spins which are all set to $+$. TCA evolve with different ε. The influence arrives through East and North boundaries and changes the internal lattice state. The minimal subordering gained for $\varepsilon = 0.800$ is $m' > 0.12$. $L = 300$.

A. Quasilocality

Quasilocality on the lattice systems means that any finite-volume expectations do not depend on spins which are sufficiently distant. On the large lattice, $L = 300$, we test the influence of distant spins on the magnetization of a spin $\mathcal{O}$, which is located at the lattice center. The experiment goes as follows. The TCA system initiated with all spins up is left to reach its stationary state at the given stochastic parameter ε. Then, the periodic boundary conditions are changed into the fixed boundary of all spins up. After allowing the system to reach the stationary state with the new boundaries, we begin to measure the magnetization of all spin sites located along the central line of a lattice. The results are presented in Fig. 9.

In this experiment we are able to estimate the difference between the magnetization of the spin $\mathcal{O}$ on a periodic lattice $m(\sigma_\mathcal{O})$ and the magnetization of the spin $\mathcal{O}$ for fixed boundary condition $m(\sigma_\mathcal{O}|(+))$. In Fig. 9 arrows mark the minimal distance between the obtained magnetization value and the value observed in the stationary periodic state.

It is easy to see the conditions under which there is no observed influence of the surrounding boundaries:

(a) before the phase transition, when $\varepsilon > 0.84$, then $m(\sigma_\mathcal{O}|(+)) = m(\sigma_\mathcal{O})$,

(b) after the phase transition, when $\varepsilon < 0.72$, then $m(\sigma_\mathcal{O}|(+)) = m(\sigma_\mathcal{O}) = 0$.

However, if the plus boundary is switched to the minus boundary, then $m(\sigma_\mathcal{O}|(-)) = -m(\sigma_\mathcal{O})$. Hence, in a rather large interval of ε, there is observed influence of distant spins on stationary states generated on the large lattice.

B. Large deviations

The stationary measures arising from any Markov process could be Gibbsian measures if the relative entropy density

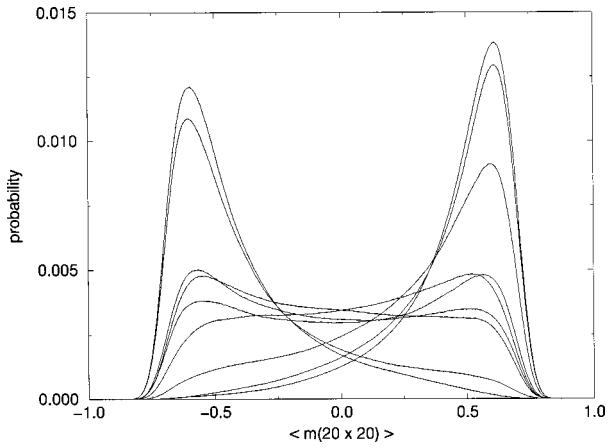

FIG. 10. Probability distribution of blocks with 20×20 size magnetized at a given value. $\varepsilon=0.820$ and $L=100$. Each curve represents a histogram of the results observed in subsequent 10 000 time steps.

$i(\mu|\nu)$ between different stationary measures μ and ν originating from the same interactions is zero. If $i(\mu|\nu)>0$, then both measures are non-Gibbsian [6,15]. The large deviation theorems [15] provide the powerful tool to estimate $i(\mu|\nu)$. Namely, if μ_- and μ_+ are two stationary TCA measures corresponding to $(-)$ and $(+)$ phases, then the relative entropy density between these two measures $i(\mu_-|\mu_+)$ can be extracted from the probability that the large area of spins with negative magnetization occurs in the stationary state described by the μ_+ measure. The result $i(\mu_-|\mu_+)>0$ means that these measures have the probability of large deviations, which is ''too small'' for Gibbsianness.

From computer experiments we collect data on the magnetization of square blocks of the size $l\times l$. Then, using the formula

$$i_l(\mu_-|\mu_+)=\lim_{l\to\infty}\frac{1}{l^2}\ln \text{Probability}_{\mu_+}\{m(\sigma_{l\times l})<0\} \tag{17}$$

we estimate the limit

$$i(\mu_-|\mu_+)=\lim_{l\to\infty} i_l(\mu_-|\mu_+).$$

As was mentioned earlier, configurations, representatives of critical stationary states, contain long-living and large objects: domains of one phase. In Fig. 10 we present the probability distribution of square blocks of 20×20 spins at a given magnetization, found after averaging over subsequent 10 000 time steps. It appears that the total magnetization changes over a long period of time. This long time correlation implies difficulties in giving a reliable value for the limit of $i_l(\mu_-|\mu_+)$ as $l\to\infty$. In Fig. 11 we present our attempts to provide the limit value for $i(\mu_-|\mu_+)$. If blocks of $l<40$ are considered, then i_l extrapolated linearly would give zero for $l>50$. Since processing data for large blocks demands much more computer time, we skip some l points and start our observations at blocks, with sizes $l>60$. The data collected for the blocks : $60<l<70$, indicate that i_l would attain zero when blocks are of a size $l>80$. Concluding our trials, we

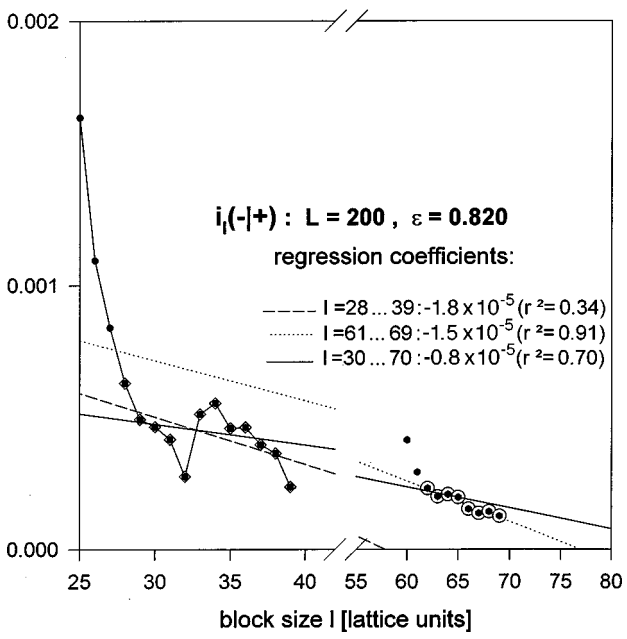

FIG. 11. Decay of relative entropy density $i_l(-|+)$ indicated by blocks of $l<40$ points at $l>50$ as the block size for which $i_l(-|+)\approx0$ (dashed line with regression $-1.8\ 10^{-5}$). The data collected for $l=61,\ldots,70$ (dotted line with regression $-1.5\ 10^{-5}$) yield different (larger) block size for i_l to attain zero. The numbers in ( ) mean the correlation coefficient r^2 for the presented data.

can say that with the increase of the block size the decay of the relative entropy density slows down.

Fortunately, when we shift a little from the critical point preserving the nonergodic property of a system, we can obtain the value for the relative entropy density. The thermodynamic state is in the nonergodic regime if the change of the phase, which is placed as the boundary, switches the phase of the inside state, see [15]. The mean magnetization of a state on a periodic lattice obtained at $\varepsilon=0.800$ is zero. If the $(+)$ boundary is put in place of the periodic one, then the mean magnetization becomes positive. Figure 12 gives estimates for $i_l(\mu_-|\nu)$, where ν is the stationary measure for $\varepsilon=0.800$. Extrapolating these results, we conclude that at $l=105$ the relative entropy density would reach zero. However, this block size is greater than the lattice size considered in this experiment; therefore, the relative entropy density between stationary measures of Toom cellular automata evolving in the critical regime on the periodic lattice is positive.

V. CONCLUSIONS

The critical regime in TCA manifests itself in the way characteristic to any thermodynamic system, i.e., by the rapid increase in the two-point correlation function of spin states, if the temperature, like stochastic parameter, is fine tuned. However, analogies with equilibrium systems must be treated with great care, especially when the stochastic parameter ε is defined at the microscopic scale only, and cannot be easily related to the macroscopic temperature.

On the stationary configurations of TCA we observe the process of emergence of islands of one phase. The mechanism behind this phenomenon is the following: once the line

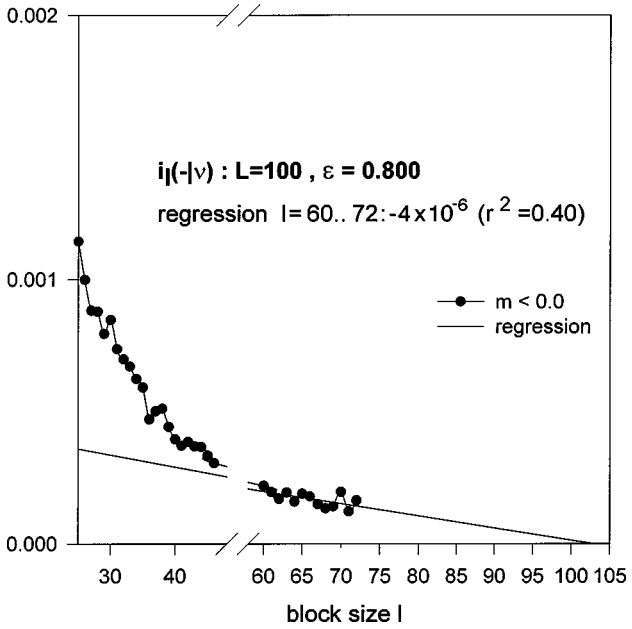

FIG. 12. Density of the relative entropy between stationary measures μ_- and ν, which is the measure of TCA shifted a little from the critical point. Linear regression indicates $i_l=0$ at $l>105$. This is impossible on the lattice of size $L=100$. The number in ( ) mean the correlation coefficient r^2 for the linear fit.

of aligned spins located orthogonally to North-East direction is established, the dynamics proceeds to spread the phase in the interior below this line, i.e., towards South and West. The island formed in this process attains the characteristic shape of the scaled basic neighborhood. This characteristic shape allows the long existence of any island. The process involved in formation of steady clusters of one phase seems to be similar to that which governs the critical behavior in all systems of the Ising type. However, in case of TCA the specific conditions necessary to establish a steady island make the total probability that a cluster of opposite phase forms too small for Gibbsianness.

On one hand, the static critical exponents found by us, $\nu=0.85$, $\beta=0.12$, and $\gamma=1.59$ are roughly consistent with the hyperscaling relation $2\beta+\gamma=2\nu$, which is typical for fluctuation dominated transitions. On the other hand, the specific-heat property indicates the diffusive mechanism of the phase transition. These two mechanisms govern together the phase transition result that the values of the particular exponents of Toom cellular automata are distinct from those corresponding to Ising system. Moreover, TCA seem to not belong to the weak-Ising universality class, either. However, the values of TCA exponents are close to the values found in the synchronized CML system.

In general, deriving accurate numerical estimates for quantities, which characterize the critical regime of an extended dynamical system, is a difficult task; see [8] and references given therein. We believe that the employed methodology here is reliable. Estimates of critical exponents ν and β are derived from at least three quantities. Only evaluation of the γ static exponent is based on the properties of one function. Although the statistical errors accompanying measured observables are large, the correlation coefficients for our linear fits are always very close to 1. This fact additionally ensures accuracy of the presented results. However, these results could be easily improved if one performs experiments which provide access to the critical point closer than we have done.

Our considerations on Gibbsianness are also accompanied by relatively large errors. In numerical studies we have to balance the influence of periodicity of the system and computer efficiency. The effect of the system periodicity is that a self-created island of one phase (which appears at random) can dominate the stationary state for a long time. This is so until the next island emerges and takes over the domination in the configuration. The way to weaken this constant process of changes in the stationary state is to consider larger blocks on the larger lattice for longer times of observations. However, the computer efficiency goes down rapidly when the system size increases. The other way of improving reliability of our estimates consists of searching parallelly for densities of the relative entropy $i(\mu_-|\mu_+)$ in Toom CA and Domany CA. This is our program for the future.

This research was supported by Polish Committee of Research KBNPB0273/P03/99/16. Simulations were partially performed in the TASK-Academic Computer Center in Gdansk, Poland.

[1] K. Binder, in *Monte Carlo Methods in Statistical Physics* (Springer-Verlag, Berlin, 1979).
[2] D. Stauffer, *Annual Reviews of Computational Physics* (World Scientific, Singapore, 1994), Vols. I–II.
[3] J. J. Binney, N. J. Dowrick, A. J. Fisher, and M. E. J. Newman, in *The Theory of Critical Phenomena* (Oxford University Press, Oxford, 1992).
[4] Ch. H. Bennett and G. Grinstein, Phys. Rev. Lett. **55**, 657 (1985).
[5] J. L. Lebowitz, Ch. Maes, and E. R. Speer, J. Stat. Phys. **59**, 117 (1990).
[6] Ch. Maes and K. Vande Velde, Physica A **206**, 587 (1994).
[7] J. Miller and D. A. Huse, Phys. Rev. E **48**, 2528 (1993).
[8] P. Marcq, H. Chate, and P. Manneville, Phys. Rev. Lett. **77**, 4003 (1996); Phys. Rev. E **55**, 2606 (1997).
[9] F. J. Alexander, I. Edrei, P. L. Garrido, and J. L. Lebowitz, J. Stat. Phys. **68**, 497 (1992).
[10] Ch. Maes and K. Vande Velde, Commun. Math. Phys. **189**, 277 (1997).
[11] A. L. Toom, N. B. Vasilyev, O. N. Stavskaya, L. G. Mityushin, G. L. Kurdyumov, and S. A. Prigorov, in *Stochastic Cellular Systems: Ergodicity, Memory, Morphogenesis*, edited by R. L. Dobrushin, V. I. Kryukov, and A. L. Toom (Manchester University Press, Manchester, 1990).
[12] D. Makowiec, Phys. Rev. E **55**, 6582 (1997); Acta Phys. Pol. B **29**, 1599 (1998).
[13] D. Makowiec, Phys. Rev. E **56**, 5195 (1997).
[14] T. M. Liggett, *Interacting Particle Systems* (Springer-Verlag, Berlin, 1985).
[15] A. C. D. van Enter, R. Fernandez, and A. D. Sokal, J. Stat. Phys. **72**, 879 (1993).

[16] R. Fernandez, Physica A **263**, 117 (1999).
[17] G. Grinstein, C. Jayaparash, and Ye Hu, Phys. Rev. Lett. **55**, 2527 (1985); B. C. S. Grandi and W. Figueiredo, Phys. Rev. E **53**, 5484 (1996).
[18] Ya G. Sinai, *Theory of Phase Transitions: Rigorous Results* (Academiai Kiadó, Budapest, 1982); M. Zahradnik, Chem. Phys. **93**, 559 (1994).
[19] G. Giacomin, J. L. Lebowitz, and Ch. Maes, J. Stat. Phys. **80**, 1375 (1995).
[20] K. Binder, Z. Phys. B **43**, 119 (1981).
[21] D. Landau, in *Proceedings of the 8th Joint EPS-APS International Conference on Physics Computing*, edited by P. Borcherds, M. Bubak, and A. Maksymowicz (Academic Computer Centre Cyfronet, Krakow, 1996).
[22] A. Munster, *Statistical Thermodynamics* (Springer-Verlag, Berlin, 1969), Vol. 1.
[23] J. Klamut, K. Durczewski, and J. Sznajd, *Introduction to Physics of Phase Transitions* (Polish edition by Zakład Narodowy im. Ossolińskich, Wrocław, 1979).